

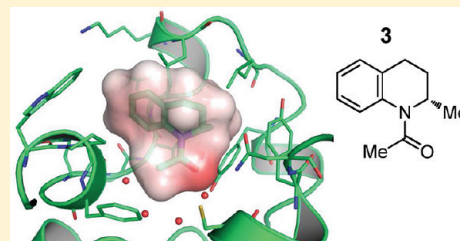
Fragment-Based Discovery of Bromodomain Inhibitors Part 1: Inhibitor Binding Modes and Implications for Lead Discovery

Chun-wa Chung,^{*,†} Anthony W. Dean, James M. Woolven, and Paul Bamborough[†]

Computational & Structural Chemistry, Molecular Discovery Research, GlaxoSmithKline R&D, Medicines Research Centre, Gunnels Wood Road, Stevenage, Hertfordshire SG1 2NY, U.K.

Supporting Information

ABSTRACT: Bromodomain-containing proteins are key epigenetic regulators of gene transcription and readers of the histone code. However, the therapeutic benefits of modulating this target class are largely unexplored due to the lack of suitable chemical probes. This article describes the generation of lead molecules for the BET bromodomains through screening a fragment set chosen using structural insights and computational approaches. Analysis of 40 BRD2/fragment X-ray complexes highlights both shared and disparate interaction features that may be exploited for affinity and selectivity. Six representative crystal structures are then exemplified in detail. Two of the fragments are completely new bromodomain chemotypes, and three have never before been crystallized in a bromodomain, so our results significantly extend the limited public knowledge-base of crystallographic small molecule/bromodomain interactions. Certain fragments (including paracetamol) bind in a consistent mode to different bromodomains such as CREBBP, suggesting their potential to act as generic bromodomain templates. An important implication is that the bromodomains are not only a phylogenetic family but also a system in which chemical and structural knowledge of one bromodomain gives insights transferrable to others.



INTRODUCTION

The epigenetic mechanisms that control gene expression offer exciting and largely untapped possibilities for drug discovery.^{1–3} These mechanisms include methylation of DNA as well as the post-translational modifications (PTMs) of the nucleosome that govern chromatin remodeling and transcription. Histone PTMs are dynamically added and removed by a range of enzymes, many of which have been the target of drug discovery efforts, including acetyltransferases, deacetylases, and methyltransferases.⁴ The reader or effector domains that recognize these modifications have been less intensively pursued as therapeutic targets.^{5,6} As mediators of protein–protein interactions, the general perception is that they may be poorly tractable to small-molecule intervention. Recent discoveries of low-molecular-weight inhibitors of bromodomains^{7–13} and MBT reader domains,^{14,15} however, challenge this view.

One histone PTM that regulates DNA replication is lysine acetylation,¹⁶ modulated through histone deacetylases and acetyltransferases (HDACs and HATs). While there are many domain classes that recognize lysine methylation, such as chromodomains and Tudor domains, the bromodomain is the sole reader module for acetyl-lysine (AcK).⁶ These small domains (~110 residues) are found within many chromatin-associated proteins such as HATs and are part of the machinery that ensure the fidelity of interpreting the so-called “histone code”. There are at least 56 bromodomains in 42 proteins encoded by the human genome.³ Occasionally, two or more modules occur in a single polypeptide, as in the BET family of tandem bromodomain-containing proteins: BRD2, BRD3, BRD4, and BRDT.¹⁷

Blocking the acetyl-lysine binding site of bromodomains prevents recognition of acetylated histone tails and alters the process of chromatin remodeling. Small molecules that prevent histone binding *in vitro* can produce profound *in vivo* biological responses. The most potent and selective bromodomain inhibitors disclosed to date (I-BET and JQ1) target the BET bromodomains. Prophylactic and therapeutic dosing of I-BET762 dramatically suppressed cytokine expression and promoted survival in an acute murine model of LPS induced endotoxin shock.⁹ Administration of JQ1 in two mice xenograft models of a rare, rapidly fatal, NUT midline carcinoma significantly inhibited tumor growth.¹¹ As bromodomains are involved in the regulation of many genes, the therapeutic potential of inhibitors is likely to span other disease areas. For example, in addition to links to oncology and inflammation, members of the BET family have roles in adipogenesis and viral infection.^{1,18} Indeed, compounds related to I-BET762 upregulate ApoA1,¹⁰ supporting their additional potential as metabolic agents.

Both I-BET and JQ1 originated from phenotypic cellular screens. To discover new classes of bromodomain inhibitors, we adopted a structure-based design approach exploiting the wealth of public and proprietary structural information. Numerous bromodomain crystal structures have been reported, including those of all the BET family members.^{19–24} These show a common fold of four antiparallel α helices, with the peptide recognition pocket located within loops at one end of the helical bundle.²⁵ Most have been crystallized without a

Received: August 16, 2011

Published: December 5, 2011

binding partner because few cognate peptides and even fewer small molecule ligands are known. Consequently, although the architecture of these domains is well established, understanding of the elements necessary to achieve high affinity binding is only beginning to emerge.

At the time of submission of this manuscript and prior to very recent online publications,^{26,27} only a handful of small molecule inhibitors had been reported and even fewer had published crystallographic binding modes. Aside from analogues of the benzodiazepine I-BET762,^{9,10} the similar thienodiazepine JQ1,¹¹ and fragments 6 and 7²⁴ (which will be discussed in greater detail below), only two bromodomain X-ray complexes of other chemotypes had been reported (Figure 1).

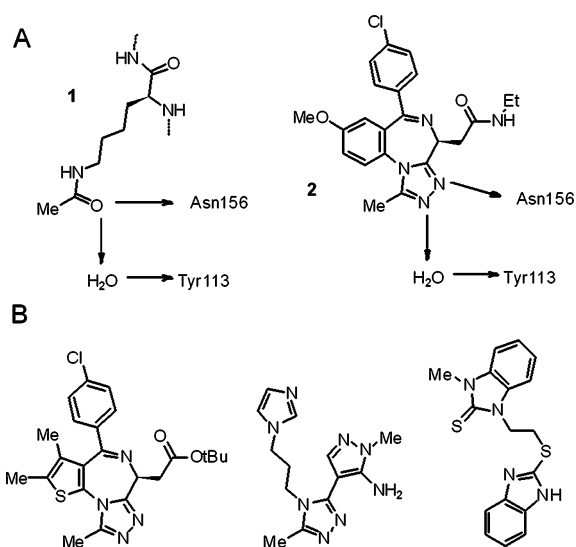


Figure 1. (A) The benzodiazepine 2 is a mimic of acetyl-lysine 1. Arrows show conserved hydrogen-bonds to the AcK-site asparagine (Asn156 in BRD2) and bridging water. Methyl groups of the two compounds occupy a small lipophilic pocket. (B) All other compounds crystallized in bromodomains to date (excluding analogues of 2, fragments 6 and 7, and 3,5-dimethylisoxazoles^{26,27,35}). From right to left: JQ1 with BET bromodomains,¹¹ triazole with BAZ2B bromodomain,²⁴ reported benzimidazole with BRD2 bromodomain.¹²

We were fortunate to have access to bromodomain crystal structures in which the AcK pocket is occupied by small molecules from multiple chemical series, including benzodiazepines such as I-BET762 and others yet to be disclosed. These show the detailed interactions by which the bromodomain recognizes small molecules. The clustering of compounds in the AcK site suggested that fragment-based drug discovery (FBDD) could be used to pursue new classes of inhibitors. This approach seeks to find small (MW < 250 Da) but efficient compounds as starting points for optimization by high-concentration screening.^{28–30} FBDD has several advantages: one is that because the size of fragment chemical space is far smaller than that of larger molecules, smaller screening sets are needed to discover hits.³¹ A disadvantage is that the interactions are weak and may be difficult to distinguish from noise and artifacts. FBDD has been attempted previously for bromodomains using NMR as the detection tool, and fragments that bind to PCAF^{7,32} and CREBBP^{8,13} were found. In one study,⁸ a targeted screening set of compounds closely related to acetyl-lysine, containing a $-\text{NHCOCH}_3$ group linked to aromatic rings, was screened in a 2D $^1\text{H}-^{15}\text{N}$ -HSQC

assay. Hits with potency of $\sim 20 \mu\text{M}$ were identified and modeled into the binding site with the help of NMR data. Binding mode prediction without crystallography is challenging because of the solution flexibility of the binding site loops and recent insights that key interactions are mediated by water molecules, which are more difficult to place by NMR techniques. The scarcity of bromodomain/small molecule X-ray complexes in the public domain also hinders reliable modeling.

Here we report the results from screening a chemically diverse, focused fragment set of putative AcK mimetics, assembled using an extensive proprietary X-ray structural knowledge-base, against the BET bromodomains. Multiple chemically diverse hits have been identified and confirmed using orthogonal methods. Most significantly, the binding modes of over 40 of these have been elucidated by X-ray crystallography. We present examples of some of the ways in which diverse chemical templates can antagonize the bromodomain–AcK interaction. A following report exemplifies the optimization of a fragment hit through structure-based design to give a series of efficient compounds with cellular anti-inflammatory activity.²⁶

RESULTS

Fragment Screening. Since discovering the BZD inhibitors of the BET family bromodomains using an Apo-A1 upregulator assay,^{9,10} we have found additional chemical series by a number of complementary approaches including high-throughput biochemical screening and rational design. The binding of diverse chemotypes has been characterized by X-ray crystallography. This structural knowledge base provides an invaluable resource for drug discovery. We have found that inhibitors showing little chemical similarity to each other share common binding features. For example, I-BET762 (2) shows no obvious resemblance to the AcK side chain that binds within the same pocket (Figure 1A). However, both ligands form hydrogen bonds to two highly conserved side chains: directly to an asparagine (Asn156 in BRD2) and indirectly via water to a tyrosine (Tyr113 in BRD2). This bridging water molecule is part of an extensive hydrogen-bonded water network buried deep within the acetyl-lysine site. Similarly, the methyl groups of both ligands occupy a small pocket formed in part by the side chain of Phe99. This molecular mimicry is illustrated in Figure 1A. Conserved residues responsible for these interactions are highlighted in the phylogenetic tree and alignment (Figure 2A,B).

Upon the basis of observations from our structural knowledge-base, we assembled and screened a focused set of fragments that contain an AcK-mimetic. Each has hydrogen-bonding functionality and a small alkyl substituent as indicated in Figure 1A. The GlaxoSmithKline compound collection and externally available databases were searched for molecules that satisfied this arrangement of features. Screening was carried out against BRD2, BRD3, and BRD4 using a fluorescence anisotropy (FA) assay. Compounds were screened in duplicate at $200 \mu\text{M}$, a relatively low concentration for a fragment screen, but the FA assay proved a robust, low-resource, and sensitive platform able to identify weak fragment hits (Supporting Information, Figure S1). Of 1376 compounds tested, 132 showed >30% displacement of the fluorogenic ligand from at least one of the tandem BET proteins. Hits were subsequently retested at full curve in the FA assay and in a TR-FRET peptide-displacement assay.

Fragment Crystal Structures. Direct target engagement was confirmed using X-ray crystallography. Compounds were soaked at high concentration into *apo* crystals of the N-terminal

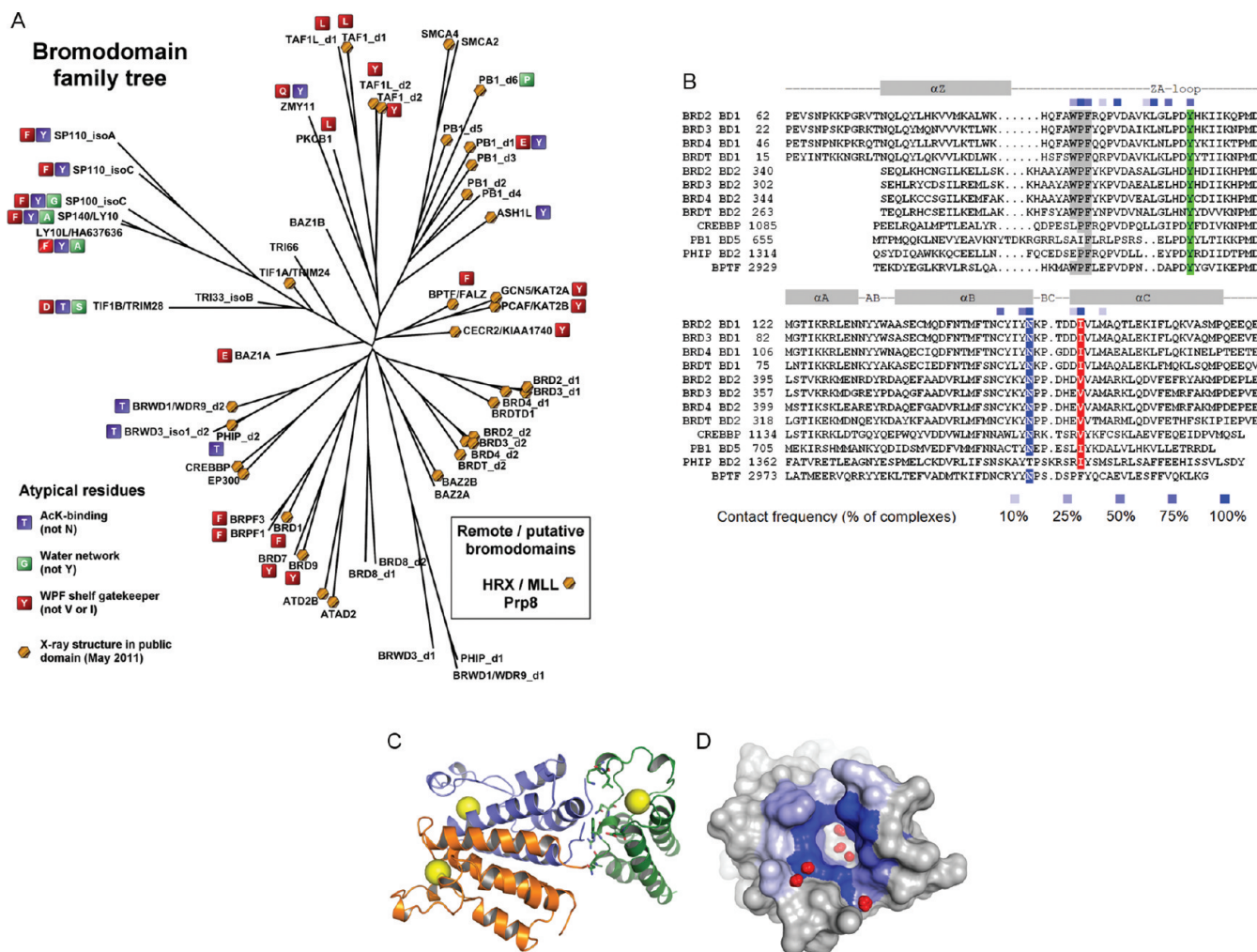


Figure 2. Sequence and structural relationships. (A) Bromodomain phylogenetic tree³ showing those for which X-ray structures are publicly available. Key residues of “typical” bromodomains are marked: blue = AcK-binding asparagine (BRD2 Asn156); green = water-binding tyrosine (BRD2 Tyr113); red = gatekeeper (BRD2 Ile162).¹⁰ (B) Sequence alignment of several bromodomains. Conserved residues are indicated (colored as in Figure 2A, and gray = WPF motif, BRD2 97–99). Above the alignment, colored boxes show fragment contact frequency in 40 X-ray complexes, scaled from white (never) to dark-blue (100%). (C) The structure of the asymmetric unit of BRD2 BD1 (chain A blue, chain B orange, chain C green). Yellow spheres are AcK sites. (D) Surface of BRD2 BD1, colored by contact frequency as in Figure 2B. Red spheres show conserved water clusters described in the text.

bromodomain of BRD2 (BRD2-BD1). This C2 crystal system contains three molecules in the asymmetric unit (chains A–C, Figure 2C). Chains A and B form an extensive parallel interface involving the length of the B and C helices of both helical bundles. Chain C has a relatively small interface between its ZA loop and the N-terminus of chain A. As residues of the ZA loop form part of the binding site, this can hinder access of larger molecules to the acetyl-lysine pocket of chain C. The fragments, however, were small enough to show consistent occupancy and binding interactions at all three sites.

The robustness of the crystal system allowed many different BRD2/fragment complex structures to be solved. Forty of these complexes with diverse fragments bound have been analyzed. First we examined which of the hydrogen-bonding interactions (arrows in Figure 1A) are essential. The fragment atom closest to the bridging water associated with Tyr113 is invariably nitrogen or oxygen, satisfying its H-bonding potential. Rarely, the closest ligand atom to Asn156 is carbon, but in these cases this interaction is usually longer range (Figure 3). Even when both of these interactions involve ligand heteroatoms, the

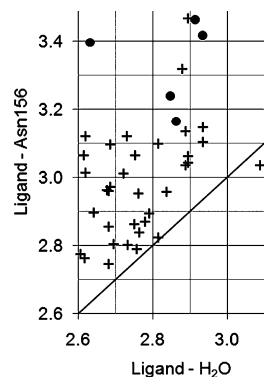


Figure 3. Plot of the distance between the ligand and the Asn156 side chain nitrogen against that between the ligand and the bridging water molecule for 40 diverse BRD2/fragment complex structures. Symbols show the element of the ligand heavy atom closest to Asn156 (crosses = nitrogen or oxygen, circles = carbon).

fragment is almost always closer to the bridging water than to Asn156. Altogether, this suggests that the H-bond interaction

with the bridging water dominates that with the asparagine but that both influence ligand positioning. We also analyzed the positions of bound water molecules within the complexes. In addition to the deeply buried water molecules within the AcK pocket, three others were consistently conserved (Figure 2D). Two waters cap the N-terminus of the C-helix, H-bonding to the backbone NH atoms of Asp161 and Ile162, while the third caps the C-terminus of the B-helix, H-bonding to the carbonyl oxygen of Tyr155.

In the sequence alignment of Figure 2B and the surface representation of BRD2-BD1 (Figure 2D), each residue is colored by its frequency of fragment binding (the fraction of the 40 representative structures in which the residue interacts with the bound fragment with a heavy-atom distance ≤ 4.5 Å). Figure 2D therefore summarizes the preferred interaction surface and low-energy water molecules involved in efficient AcK-mimetic binding to BRD2-BD1. An alignment of this domain with other bromodomains within and beyond the BET family (Figure 2A,B) highlights the preservation of most of the key interaction residues between members of this target class. "Typical" bromodomains have a conserved tyrosine (Tyr113 in BRD2) to coordinate the active site bridging water molecule, an asparagine equivalent to Asn156, and valine or isoleucine at the "gatekeeper" position equivalent to Ile162, as well as other conserved positions near the AcK site. Our interaction analysis suggests that our fragments are unlikely to discriminate between BET family members, a conclusion confirmed by the strong correlation of activities found (Supporting Information, Figure S1). Unsurprisingly, structures of pan BET compounds within different BET family bromodomains display indistinguishable binding modes.¹⁰

We next discuss the detailed binding modes of some representative fragments 3–7 (Table 1). All bind in the acetyl-

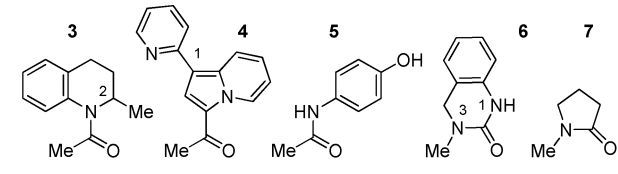
complex in the same orientation as Figure 4A, the highly homologous BRDT bound to an acetylated histone H4 peptide.²³ In accord with the design strategy of the focused set, the amide substituent of 3 mimics the acetyl carbonyl of the AcK side chain, forming the interactions with Asn156 and the bridging water molecule described earlier. Its methyl group also binds in the same pocket as the AcK methyl, adjacent to Phe99. The THQ ring fills the lipophilic part of the pocket, with the aromatic portion between Pro98 and Leu108 and the aliphatic part of the ring lying against the gatekeeper residue Ile162. The *S*-configuration of the C2 atom of the THQ ring places the 2-position methyl group into another small lipophilic pocket which is not occupied by the acetyl-lysine side chain. This makes hydrophobic contacts with the side chains of Val103, Leu108, Leu110, Tyr113, and Tyr155. The hydrogen atom at the THQ ring 2-position points directly toward the carbonyl oxygen of the Asn156 side chain. The distance between the C2 atom and Asn156 is 3.3 Å, close enough that the methyl of the *R* enantiomer would clash and prevent binding.

The THQ template is more rigid and makes more interactions than the native AcK side chain and is an appealing starting point for chemistry because of its chemical tractability and high binding efficiency. It achieved almost 50% inhibition at 100 μ M in the FA assay, giving it an approximate IC_{50} of 100 μ M and ligand efficiency (LE) of around 0.39 (Table 1), which compares favorably to the next fragment we will describe.

1-(1-(Pyridin-2-yl)indolizin-3-yl)ethanone. Fragment 4 is a more potent hit than 3 (Table 1), doubtless because of its greater size. Crystallography shows that 4 has a similar binding mode to 3, utilizing a methyl ketone template to mimic the acetyl-lysine headgroup (Figure 4C). Aside from this motif, the remaining interactions with the protein are all lipophilic in nature. The indolizine ring fulfills an analogous role to the saturated part of the THQ ring, sandwiched between the gatekeeper Ile162 and Leu108/Leu110. The 2-pyridyl substituent at the 1-position of the indolizine fills a further lipophilic space between Leu108 and the side chains of Trp57 and Pro58 of the WPF motif. The only accessible polar atom is the pyridyl nitrogen. No protein atoms or visible water molecules are sufficiently close to contact this nitrogen, so the pyridine may adopt a position rotated by 180° from that shown. As 4 had good potency and ligand efficiency ($IC_{50} \approx 2$ μ M, Table 1), it was tested in a cellular inflammation assay. We used an IL-6 inhibition assay, as this cytokine has been shown to be regulated by BET inhibitors.⁹ Surprisingly for such a small compound, it showed reproducible inhibition of IL-6 release from LPS-stimulated PBMC cells, with $IC_{50} \approx 14$ μ M (pIC_{50} 4.9 \pm 0.2, mean of $n = 4$).

Acetaminophen (Paracetamol). After viewing the essential binding features of 4, we tested one of the most commonly used drugs, acetaminophen (paracetamol, 5), for its ability to bind to the BET bromodomains. While acetaminophen was found to be a very weak fragment, with an undetectable inhibition in the FA assay at 100 μ M, its structural similarity to 4 suggested that it could satisfy many of the common features required for occupation of the acetyl-lysine pocket. To test this, crystals of BRD2-BD1 were soaked with high concentrations (~ 10 mM) of 5. The resulting 1.91 Å structure (Figure 4D) shows unequivocally that 5 binds in a consistent and predicted fashion within the AcK pocket of all three chains of BRD2-BD1. Gratifyingly, its binding mode overlays perfectly with that of compound 4 (Figure 4C,D). The phenyl ring of 5 follows the path of the bound acetyl-lysine side chain, sandwiched between the lipophilic side chains of Ile162 on one side and

Table 1. Molecular Weight and Activity of Fragments 3–7^a



Compound	3	4	LE of 4	5	6	7	
MW	189	236		151	162	99	
BRD2	44%	12.6 μ M	0.37	11%	12%	<5%	
FA @ 100 μ M	BRD3	44%	6.3 μ M	0.40	7%	14%	<5%
	BRD4	42%	10.0 μ M	0.38	<5%	9%	<5%
TR-FRET @ 50 μ M	BRD2	44%	2.0 μ M	0.43	6%	23%	<5%
	BRD3	29%	2.5 μ M	0.43	19%	22%	<5%
	BRD4	35%	2.0 μ M	0.43	12%	25%	<5%

^aActivities are expressed as %I at the top screening concentration (100 μ M for the FA assay and 50 μ M for the TR-FRET assay) or as IC_{50} (mean of at least four replicates) for 4. Ligand efficiency (LE) of 4 is shown: $LE \approx 1.37(pIC_{50}/\text{number of heavy atoms})$. The LE of 3 \approx 0.39, based on $IC_{50} \approx 100$ μ M.

lysine pocket of BRD2-BD1 as intended, mimicking the interactions highlighted in Figure 1A.

N-Acetyl-2-methyltetrahydroquinoline. The racemic N-acetyl-2-methyltetrahydroquinoline (THQ) 3 had similar activity in the FA and TR-FRET assays (Table 1). The 2.05 Å BRD2-BD1 X-ray structure reveals the atomic details of binding to the AcK pocket, as well as that the configuration that binds is the *S*-enantiomer (Figure 4, Figure 5). Figure 4B shows the

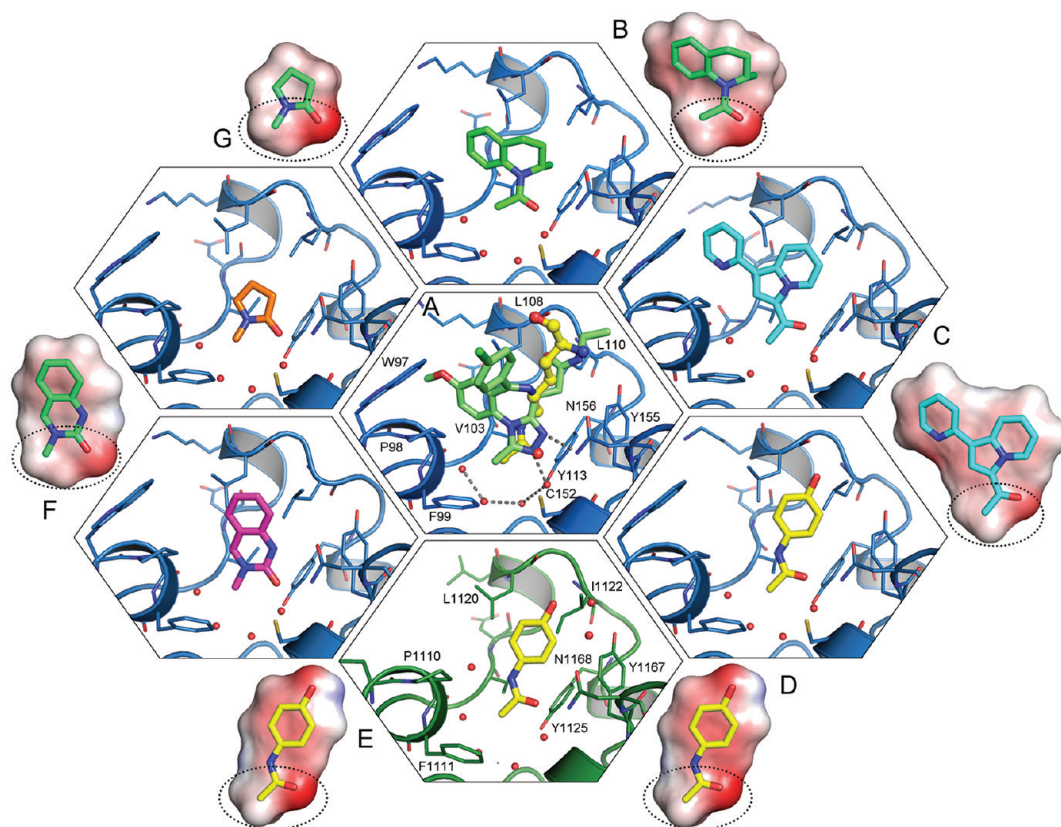


Figure 4. X-ray structures in the same orientation (with ZA loop at the back). Each complex in B–G is shown alongside the ligand molecular surface colored by electrostatic potential (red = negative, blue = positive). The part of each ligand that acts as the acetyl-lysine mimetic is circled with a dotted line. (A) Complex between BRD2-BD1 (blue) and BZD 1 (green). Acetyl lysine taken from the complex with mouse BRDT-BD1 and histone H4 (1–20, K5Ac K8Ac)²³ is shown in yellow. Four conserved water molecules are shown as small red spheres with their interactions as gray broken lines. BRD2 residue numbering is identical in Figures 2A–D,F,G. The gatekeeper Ile162 lies toward the front of the view and has been removed for clarity. (B) Complex between BRD2-BD1 and 3, the tetra-hydroquinoline (green). (C) Complex between BRD2-BD1 and 4 (cyan). (D) Complex between BRD2-BD1 and 5, acetaminophen/paracetamol (yellow). (E) CREBBP bromodomain (green) complexed with 5 (yellow). (F) Complex between BRD2-BD1 (blue) and 6 (magenta). (G) Complex between BRD2-BD1 and 7, *N*-methylpyrrolidin-2-one (orange).

Leu108 and Leu110 on the other. The phenolic oxygen of **5** extends toward the solvent region at the edge of the pocket and forms a hydrogen-bond to a water molecule, which is not well preserved within our fragment structures so its contribution to binding is doubtful.

Because of its small size, **5** only engages residues that are critically involved in acetyl-lysine recognition and which are highly conserved across the “typical” bromodomains (Figures 2C,D). This suggests it may bind in an equivalent manner to many of these. Noting that phenylacetamide-containing compounds have been shown by NMR to bind to CREBBP,⁸ we obtained a 1.81 Å X-ray structure of the CREBBP bromodomain with **5**. The binding mode observed in BRD2 and CREBBP (Figure 4E) is preserved as predicted.

3-Methyl-3,4-dihydroquinazolin-2(1*H*)-one. Fragments **3**–**5** all possess clear acetyl moieties presented on different scaffolds. The 1.91 Å structure of compound **6** illustrates that cyclization of these binding features can be tolerated and exemplifies more diverse AcK mimicry (Figure 4F). While **6** binds in a similar manner as **3**–**5**, the hydrogen-bond acceptor and methyl functional groups of **6** are linked by an additional atom incorporated into a ring. The hydrogen bond to the bridging water is satisfied by the exocyclic carbonyl of the 3,4-dihydroquinazolin-2(1*H*)-one. The resulting different vectors presented by this fragment offer opportunities for elaboration to explore

alternative parts of the site. Unlike the other fragments, **6** makes an additional hydrogen-bond donor interaction with the side chain carbonyl of the conserved Asn156 through its N1 hydrogen.

A search of the GlaxoSmithKline screening collection for analogues of compound **6** yielded several hits which were screened in the FA assays. The sulfonamide analogue **8** (Figure 6) showed detectable binding and an improvement in potency over **6** (IC₅₀ 30–40 μM against BRD2, BRD3, BRD4, corresponding to ligand efficiency LE ≈ 0.25–0.27). While this is not especially potent or efficient, it is significantly more potent than **6**, so we were curious to understand how the analogue bound. Given that the N1 proton of the 3,4-dihydroquinazolin-2(1*H*)-one ring of **8** is methylated, it would be unable to donate the hydrogen bond to the Asn156 carbonyl oxygen. Indeed, it would be expected that these two atoms would clash.

A 1.6 Å resolution crystal structure of **8** bound into the N-terminal BRD4 bromodomain was solved (Figure 6). This shows that the binding mode of **8** is similar to that of **6**, with the carbonyl of the 3,4-dihydroquinazolin-2(1*H*)-one maintaining its interaction with the bridging water molecule. The presence of the additional 1-methyl group is accommodated by a puckering movement in the ligand that moves the methyl away from the asparagine (Asn140 in BRD4). This might account for the relatively low ligand efficiency of this molecule. The morpholino sulfonamide substituent binds in the region we have termed the

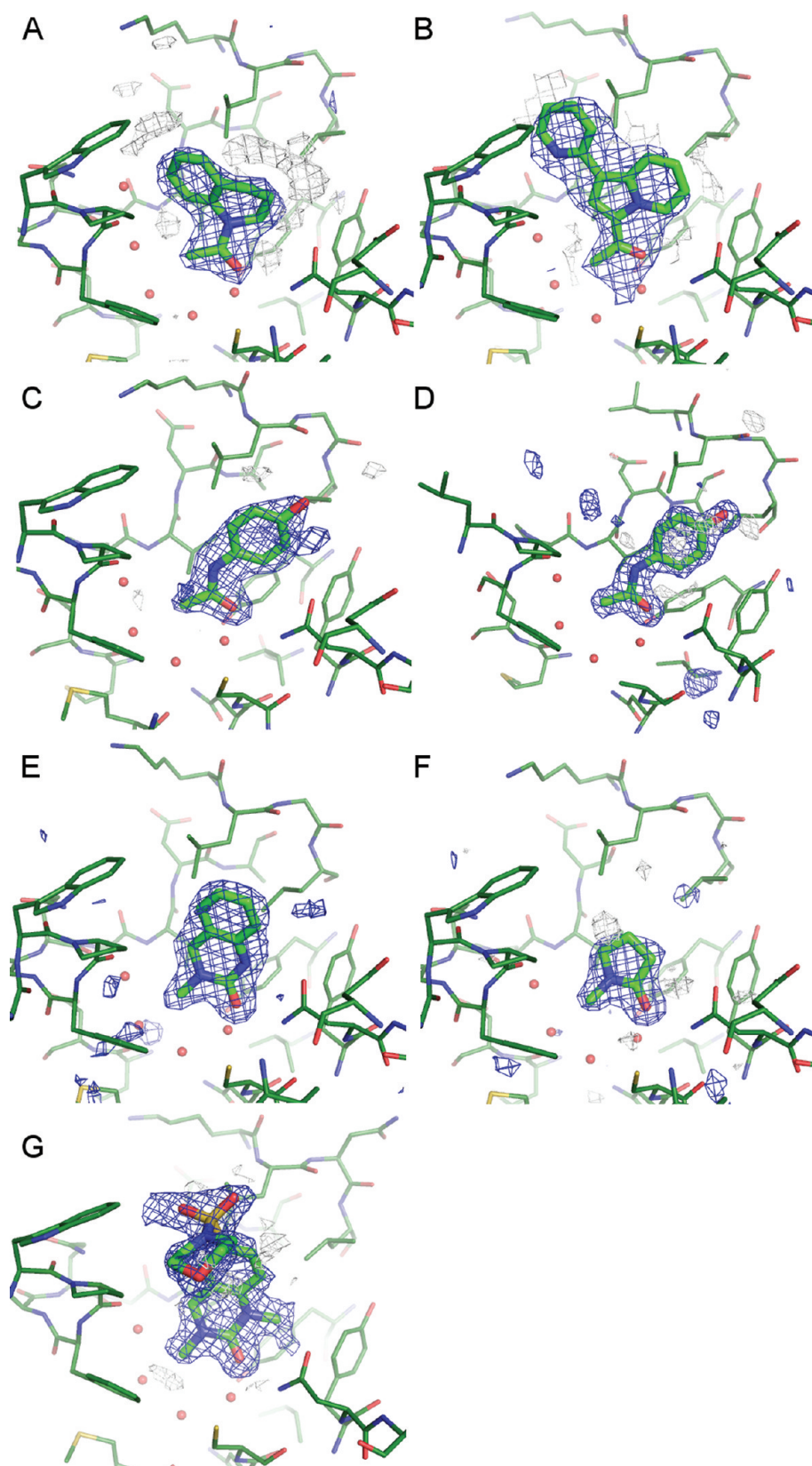


Figure 5. OMIT ($F_o - F_c$) difference maps of X-ray complexes: (A) BRD2-BD1 with **3**; (B) BRD2-BD1 with **4**; (C) BRD2-BD1 with **5**; (D) CREBBP with **5**; (E) BRD2-BD1 with **6**; (F) BRD2-BD1 with **7**; (G) BRD4-BD1 with **8**. All maps are contoured blue = 3σ , gray = -3σ , except (B) blue = 2σ , gray = -2σ , and (G) blue = 1.7σ , gray = -1.7σ .

WPF shelf, close to Trp81, Pro82, and Ile146. We have previously suggested that binding in this subpocket of the site is one way to gain increased binding affinity.¹⁰ Our interpretation of these

results is that the sulfonamide substituent of compound **8** does make this beneficial interaction but that the clashing N1-methyl substituent also imposes a significant penalty.

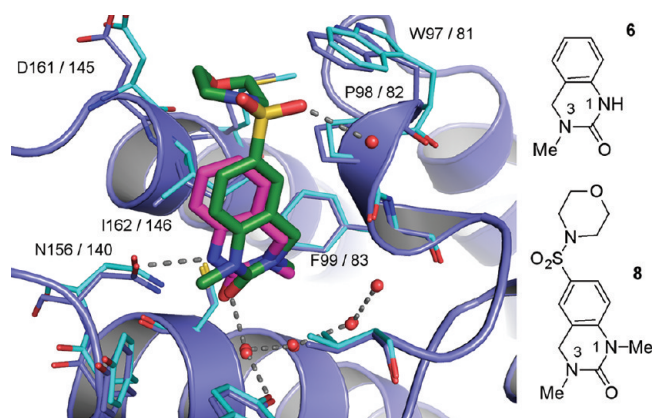


Figure 6. Structure and binding mode of **8**, an analogue of fragment **6**. Crystal structure of **8** (green) complexed with BRD4-BD1 (cyan), superimposed on that of **6** (magenta) complexed with BRD2-BD1 (blue). Hydrogen bonds are shown as gray dotted lines. Labels indicate the residue numbers of BRD2 followed by those of BRD4.

While the potency of **8** is not sufficient for it to be useful as a cellular probe of BET function, we anticipate that it could be improved (for example by removing the N1-methyl group). We use this example only to illustrate that starting from a simple fragment that occupies the AcK pocket it is possible to gain potency over the initial fragment by growing out into the surrounding areas.

The unsubstituted fragment **6** only interacts with the highly conserved features of the acetyl-lysine site. It has also been reported to bind to the acetyl-lysine pocket of CREBBP.²⁴ To our knowledge, the affinity of this interaction and the way in which it was discovered have not been published. However, comparison of the available CREBBP atomic coordinates with our BRD2-BD1 structure confirms that **6** shares a common binding mode within these two “typical” bromodomains. We anticipate that its CREBBP activity will be of similarly weak nature to that with BET but that it may be possible to build in CREBBP potency and selectivity by growing outward.

N-Methylpyrrolidin-2-one. Like acetaminophen (**4**), N-methylpyrrolidine-2-one **7** (NMP) was selected for crystallography even though it was too weak to detect in our FA assay. A 1.73 Å structure of the bromodomain of BRD2 with **7** shows an unambiguous and consistent binding mode within all three chains of the asymmetric unit (Figure 4G). It is similar to **6** in that the hydrogen-bond and methyl functional groups are separated by two ring atoms. The 6,6-fused system of **6** is replaced in **7** by a monocyclic 5-membered ring. This offers yet another set of different vectors which could be used to extend the fragment.

Like **5** and **6**, **7** is a small fragment that interacts with the conserved parts of the acetyl-lysine pocket. Accordingly, it has been shown to bind to several other bromodomains, including CREBBP, the fifth bromodomain of polybromodomain (PB1-BD5), and the second bromodomain of PHIP (PHIP-BD2).²⁴ The affinity of binding of **7** to these domains has not been reported, but is likely to be low based on its size and the very low BET potency (Table 1). BRD2-BD1, CREBBP, and PB1-BD5 are all “typical” bromodomains in which the residues binding to the AcK headgroup are highly conserved (Figures 2A,B), so a consistent binding mode of **7** to all four proteins is expected.

In contrast, the second bromodomain of PHIP (PHIP-BD2) is atypical. The analogous residue to the conserved Asn156 of

BRD2-BD1 is a threonine (T1396). The hydroxyl group of this side chain overlays approximately with the NH₂ group of the conserved asparagine of BRD2 and the typical bromodomains. However, perhaps because of the smaller size of this side chain, the carbonyl of the NMP group does not hydrogen-bond directly to the threonine: instead binding occurs via a bridging water molecule. As a result, in PHIP-BD2 there is insufficient space to accommodate the N-methyl group of the NMP in its typical position close to F1341 (the equivalent of F99 in BRD2) and a flipped orientation, where the methyl group points away from the AcK pocket, is seen (PDB entry 3mb3).²⁴

DISCUSSION

In their recent analysis, Swinney and Anthony showed that from 1999 to 2008 almost twice as many first-in-class drugs came from phenotypic screening as from targeted screening.³³ They also found that three times as many follower drugs came from targeted approaches, suggesting that these techniques are especially useful once validated drug targets have been found. While the epigenetics field is still young, it appears that it is no exception to this trend. Pioneering work in the area led to the discovery of Vorinostat (SAHA) as an inducer of cell differentiation before its histone deacetylase mode of action was known.³⁴ Similarly, the first bromodomain inhibitors were discovered as phenotypic upregulators of Apo-A1 and their targets identified subsequently.^{9–11} With data continuing to emerge supporting their potential therapeutic value,^{35,36} a move toward bromodomain-targeted drug discovery seems inevitable.

One limiting factor is the lack of known starting points for chemistry. Using structural knowledge of the essential features required for interaction at the acetyl-lysine site, fragments were selected and screened in a high-concentration competition binding assay. The success of this leads us to the conclusion that the BET family bromodomains are highly tractable to FBDD. We have identified and confirmed the binding mode of many chemically diverse acetyl-lysine mimics of the sort exemplified here. This is the first time that bromodomain X-ray complexes of molecules related to three of these (**3**, **4**, and **5**) have been reported. Against the sparse background of compound structural knowledge to date our contribution of three completely new complexes clarifying the molecular requirements for binding represents a significant addition to the literature. Each exemplifies a new way in which different scaffolds can present similar features to the bromodomain acetyl-lysine pocket.

One fragment of only 236 Da, **4**, shows micromolar affinity and measurable activity on LPS-stimulated cellular production of IL-6. For the racemic fragment **3** previously identified by NMR as a CREBBP ligand,⁸ we have resolved the stereochemical requirements for binding to the related BET bromodomain and rationalized this preference structurally by crystallography.

Although paracetamol, **5**, has been reported to act as a 26 μM COX2 inhibitor,³⁷ the biological basis for its analgesic and anti-inflammatory effects and side-effects are still a matter of much debate, and it is believed that it may act upon multiple targets.³⁸ The mechanism by which paracetamol reportedly induces differentiation of breast cancer stem cells³⁹ is unknown, but it may suggest it can influence transcriptional or epigenetic gene regulation. Inhibition of the BET bromodomains is associated with anti-inflammatory activity⁹ and with induction of differentiation in NUT midline carcinoma.¹¹ The affinities of paracetamol for the BETs are very weak (>100 μM, Table 1), so it is unlikely that any of its in vivo activity can be solely

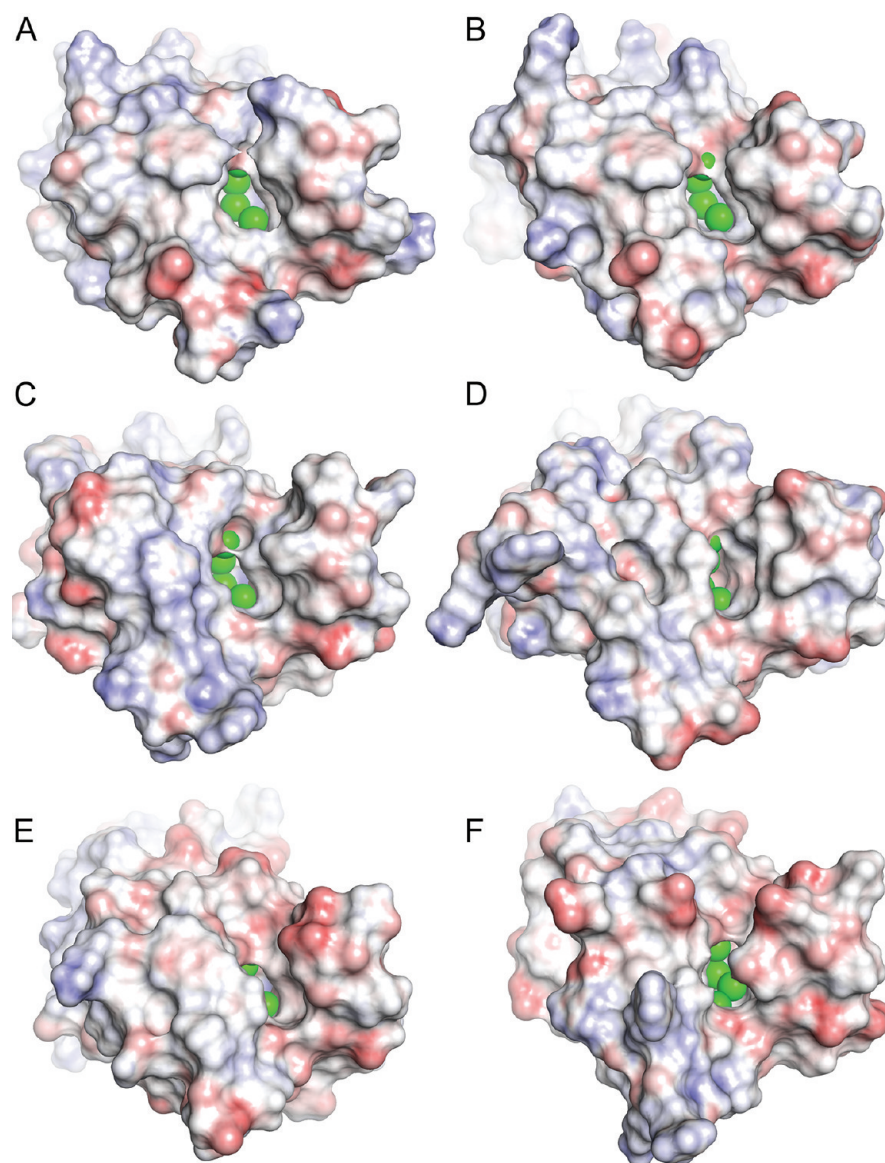


Figure 7. Electrostatic potential colored molecular surfaces of (A) BRD2-BD1, (B) BRD2-BD2, (C) CREBBP, (D) PB1-BD5, (E) BPTF, (F) PHIP BD2. Green spheres show conserved waters of the AcK-site.

attributable to binding the BET bromodomains. However, we have also demonstrated it can bind to CREBBP and is likely to interact weakly with many, even possibly all of the “typical” bromodomains (Figure 2A,B). The cumulative effect of weak engagement of multiple bromodomains, each influencing different transcriptional outcomes, is difficult to gauge but may be significant. Regardless of any physiological relevance of the bromodomain binding of paracetamol, this fragment is small and highly tractable as a starting point for the design of potent bromodomain inhibitors.

One theme emerging from this work is that small fragments can bind in similar ways to the acetyl-lysine pocket of different bromodomains. Figure 4 shows the electrostatic potential surfaces of 3–7, highlighting common characteristics which contribute to binding at the acetyl-lysine pocket. They interact with conserved waters and residues by mimicking the AcK headgroup, while lipophilic parts of the fragments engage with hydrophobic side chains. Analysis of the amino acids involved in binding fragments and the native acetyl-lysine ligand (Figure 2A,B) highlights the conservation of these residues. This

suggests that a relatively small, focused pool of fragments could be used as a common source of starting points for medicinal chemistry, and that a given fragment hit for one bromodomain has the potential to act as a lead for many.

Of course, it is not the case that a system that is tractable to fragment screening must therefore be tractable to fragment-based drug discovery. It is also necessary that the binding site permits the optimization of fragments to greater levels of potency while remaining within drug-like property space. Given the role of some bromodomain-containing proteins in fundamental cellular processes, selectivity is likely to be critical. The potential to achieve potency and selectivity depends on the nature of the pocket surrounding the fragment binding site. In bromodomains, this is formed from the long ZA and BC loops, which vary more between bromodomains than the acetyl-lysine pocket (Figure 2B, Figure 7). The range of fragments we have discovered present different vectors for exploration which could be used to target regions of greater diversity to develop increased affinity and specificity. An extensive example of this, starting from an unrelated isoxazole fragment hit, will be

reported separately in an accompanying manuscript.²⁶ Development of the *N*-acetyl-2-methyltetrahydroquinoline template (3) has yielded BET inhibitors with high levels of potency and selectivity,^{40,41} work which will also be reported separately. We have shown above another very simple example of optimization of the 3-methyl-3,4-dihydroquinazolin-2(1*H*)-one fragment 6 to an IC₅₀ of 30–40 μM using an analogue available to hand. The independent optimization of this series to give potent, submicromolar leads has very recently been reported.⁴²

CONCLUSION

The FBDD screening we described above is biased toward AcK mimetics, and it is possible that other screening strategies may discover inhibitors with different modes of binding. To investigate this, we have attempted alternative approaches, including high-throughput biochemical screening and fragment efforts using diverse compounds rather than targeted molecules, the results of which are beyond the scope of this manuscript. Significantly, the focused FBDD approach alone has enabled us to analyze 40 different small molecule bromodomain X-ray complexes, a far greater number than currently exists in the public domain Protein Data Bank. Here we have reported five complexes, three of which are chemotypes that have not been crystallized in bromodomains before. This contribution of new diverse fragments considerably extends the public crystallographic small molecule/bromodomain interaction database and should lead to increased appreciation of the variety of ways in which chemically different small molecules can make essentially the same bioisosteric interactions. In addition, we have noted that the binding modes of several fragments are preserved between bromodomains. It seems that the bromodomain family might be a true system, the members of which are related not only by evolution, fold, and function, but also by the chemical connectivity of their inhibitor space. The results are encouraging for the future of rational design of therapies targeting this protein–protein interaction and epigenetic reader class.

MATERIALS AND METHODS

Fragment Set Selection. Fragments were selected using substructural patterns designed to capture chemically diverse AcK-mimetic functional groups. The resulting list was then filtered to eliminate “nondruglike” substructures⁴³ before a careful visual assessment and application of the Rule-of-Three.⁴⁴ A further filter was used to remove compounds with predicted pK_a outside the range 5–9. The remaining fragments were clustered, and docking results used to guide selection of representative members of each cluster. Full details are given in Supporting Information and properties of the set are shown in Supporting Information, Figure S1.

Assays. The fluorescence anisotropy assay was configured as previously described.¹⁰ It measures displacement of a labeled benzodiazepine inhibitor from the BRD2, BRD3, and BRD4 acetyl-lysine binding sites (see Supporting Information). The time-resolved fluorescence resonance transfer assay was configured as previously described.¹⁰ It measures displacement of a labeled acetylated lysine histone peptide from the BRD2, BRD3, and BRD4 acetyl-lysine binding sites (see Supporting Information). The IL-6 PBMC assay measures the inhibition of cytokine release from LPS-stimulated peripheral blood mononuclear cells and is also described in Supporting Information.

X-ray Crystallography. His-tagged BRD2-BD1 (67–200), BRD4-BD1 (44–168), and CREBBP (1081–1197) were expressed in *E. coli*, purified and crystallized. Compounds were soaked into apo crystals prior to crystal freezing and data collected as described in Supporting Information. Data collection and refinement statistics are

given in Supporting Information, Table 1, and OMIT ($F_o - F_c$) maps in Figure 5.

ASSOCIATED CONTENT

Supporting Information

Supplementary methods; properties of the fragment set, BRD3/BRD4 correlation in FA assay; fluorescent ligand; X-ray statistics. This material is available free of charge via the Internet at <http://pubs.acs.org>.

Accession Codes

Coordinates have been deposited with the Protein Data Bank (4a9e, 4a9f, 4a9h, 4a9i, 4a9j, 4a9k, 4a9l) and will be released immediately on publication.

AUTHOR INFORMATION

Corresponding Author

*Phone: +44 (0)20 8047 5000. Fax: +44 1438 763352. E-mail: Chun-wa.chung@gsk.com.

Author Contributions

[†]These authors contributed equally to this work.

ACKNOWLEDGMENTS

We thank Kevin Lee, Jason Witherington, Iain Uings, Mike Hann, Pam Thomas, David Drewry, Epinova DPU, and the Departments of Biological Reagents & Assay Development and Screening & Compound Profiling.

ABBREVIATIONS USED

AcK, acetyl-lysine (AcK); ApoA1, apolipoprotein A-1; BET, bromodomain and extra-terminal; BD, bromodomain; BRD2/3/4, bromodomain-containing protein 2/3/4; BPTF, bromodomain PHD finger transcription factor; COX2, cyclooxygenase-2; CREBBP, cAMP response element-binding protein; FA, fluorescence anisotropy; FBDD, fragment-based drug discovery; HSQC, heteronuclear single-quantum correlation spectroscopy; IL-6, interleukin-6; LPS, lipopolysaccharide; NUT, nuclear protein in testis; PB1, polybromo 1; PCAF, P300/CBP-associated factor; PHIP, pleckstrin homology domain interacting protein; TR-FRET, time-resolved fluorescence resonance energy transfer

REFERENCES

- (1) Heightman, T. D. Therapeutic prospects for epigenetic modulation. *Expert Opin. Ther. Targets* **2011**, *15*, 729–740.
- (2) Denis, G. V. Bromodomain coactivators in cancer, obesity, type 2 diabetes, and inflammation. *Discoveries Med.* **2010**, *10*, 489–499.
- (3) Sanchez, R.; Zhou, M. M. The role of human bromodomains in chromatin biology and gene transcription. *Curr. Opin. Drug Discovery Dev.* **2009**, *12*, 659–665.
- (4) Kouzarides, T. Chromatin modifications and their function. *Cell* **2007**, *128*, 693–705.
- (5) Ruthenburg, A. J.; Li, H.; Patel, D. J.; Allis, C. D. Multivalent engagement of chromatin modifications by linked binding modules. *Nature Rev. Mol. Cell Biol.* **2007**, *8*, 983–994.
- (6) Taverna, S. D.; Li, H.; Ruthenburg, A. J.; Allis, C. D.; Patel, D. J. How chromatin-binding modules interpret histone modifications: lessons from professional pocket pickers. *Nature Struct. Mol. Biol.* **2007**, *14*, 1025–1040.
- (7) Zeng, L.; Li, J.; Muller, M.; Yan, S.; Mujtaba, S.; Pan, C.; Wang, Z.; Zhou, M. M. Selective small molecules blocking HIV-1 Tat and coactivator PCAF association. *J. Am. Chem. Soc.* **2005**, *127*, 2376–2377.
- (8) Sachchidanand.; Resnick-Silverman, L.; Yan, S.; Mujtaba, S.; Liu, W. J.; Zeng, L.; Manfredi, J. J.; Zhou, M. M. Target structure-based

discovery of small molecules that block human p53 and CREB binding protein association. *Chem. Biol.* **2006**, *13*, 81–90.

(9) Nicodeme, E.; Jeffrey, K. L.; Schaefer, U.; Beinke, S.; Dewell, S.; Chung, C. W.; Chandwani, R.; Marazzi, I.; Wilson, P.; Coste, H.; White, J.; Kirilovsky, J.; Rice, C. M.; Lora, J. M.; Prinjha, R. K.; Lee, K.; Tarakhovskiy, A. Suppression of inflammation by a synthetic histone mimic. *Nature* **2010**, *468*, 1119–1123.

(10) Chung, C.; Coste, H.; White, J. H.; Mirguet, O.; Wilde, J.; Gosmini, R. L.; Delves, C.; Magny, S. M.; Woodward, R.; Hughes, S. A.; Boursier, E. V.; Flynn, H.; Bouillot, A. M.; Bamborough, P.; Brusq, J. M.; Gellibert, F. J.; Jones, E. J.; Riou, A. M.; Homes, P.; Martin, S. L.; Uings, I. J.; Toum, J.; Clement, C. A.; Boullay, A. B.; Grimley, R. L.; Blandel, F. M.; Prinjha, R. K.; Lee, K.; Kirilovsky, J.; Nicodeme, E. Discovery and Characterization of Small Molecule Inhibitors of the BET Family Bromodomains. *J. Med. Chem.* **2011**, *54*, 3827–3838.

(11) Filipakopoulos, P.; Qi, J.; Picaud, S.; Shen, Y.; Smith, W. B.; Fedorov, O.; Morse, E. M.; Keates, T.; Hickman, T. T.; Felletar, I.; Philpott, M.; Munro, S.; McKeown, M. R.; Wang, Y.; Christie, A. L.; West, N.; Cameron, M. J.; Schwartz, B.; Heightman, T. D.; La, T. N.; French, C. A.; Wiest, O.; Kung, A. L.; Knapp, S.; Bradner, J. E. Selective inhibition of BET bromodomains. *Nature* **2010**, *468*, 1067–1073.

(12) Ito, T.; Umehara, T.; Sasaki, K.; Nakamura, Y.; Nishino, N.; Terada, T.; Shirouzu, M.; Padmanabhan, B.; Yokoyama, S.; Ito, A.; Yoshida, M. Real-Time Imaging of Histone H4K12-Specific Acetylation Determines the Modes of Action of Histone Deacetylase and Bromodomain Inhibitors. *Chem. Biol.* **2011**, *18*, 495–507.

(13) Borah, J. C.; Mujtaba, S.; Karakikes, I.; Zeng, L.; Muller, M.; Patel, J.; Moshkina, N.; Morohashi, K.; Zhang, W.; Gerona-Navarro, G.; Hajjar, R. J.; Zhou, M. M. A Small Molecule Binding to the Coactivator CREB-Binding Protein Blocks Apoptosis in Cardiomyocytes. *Chem. Biol.* **2011**, *18*, 531–541.

(14) Herold, J. M.; Wigle, T. J.; Norris, J. L.; Lam, R.; Korboukh, V. K.; Gao, C.; Ingerman, L. A.; Kireev, D. B.; Senisterra, G.; Vedadi, M.; Tripathy, A.; Brown, P. J.; Arrowsmith, C. H.; Jin, J.; Janzen, W. P.; Frye, S. V. Small-molecule ligands of methyl-lysine binding proteins. *J. Med. Chem.* **2011**, *54*, 2504–2511.

(15) Kireev, D.; Wigle, T. J.; Norris-Drouin, J.; Herold, J. M.; Janzen, W. P.; Frye, S. V. Identification of non-peptide malignant brain tumor (MBT) repeat antagonists by virtual screening of commercially available compounds. *J. Med. Chem.* **2010**, *53*, 7625–7631.

(16) Unnikrishnan, A.; Gafken, P. R.; Tsukiyama, T. Dynamic changes in histone acetylation regulate origins of DNA replication. *Nature Struct. Mol. Biol.* **2010**, *17*, 430–437.

(17) Florence, B.; Faller, D. V. You bet-cha: a novel family of transcriptional regulators. *Front. Biosci.* **2001**, *6*, D1008–D1018.

(18) Denis, G. V.; Nikolajczyk, B. S.; Schnitzler, G. R. An emerging role for bromodomain-containing proteins in chromatin regulation and transcriptional control of adipogenesis. *FEBS Lett.* **2010**, *584*, 3260–3268.

(19) Nakamura, Y.; Umehara, T.; Nakano, K.; Jang, M. K.; Shirouzu, M.; Morita, S.; Uda-Tochio, H.; Hamana, H.; Terada, T.; Adachi, N.; Matsumoto, T.; Tanaka, A.; Horikoshi, M.; Ozato, K.; Padmanabhan, B.; Yokoyama, S. Crystal structure of the human BRD2 bromodomain: insights into dimerization and recognition of acetylated histone H4. *J. Biol. Chem.* **2007**, *282*, 4193–4201.

(20) Umehara, T.; Nakamura, Y.; Jang, M. K.; Nakano, K.; Tanaka, A.; Ozato, K.; Padmanabhan, B.; Yokoyama, S. Structural basis for acetylated histone H4 recognition by the human BRD2 bromodomain. *J. Biol. Chem.* **2010**, *285*, 7610–7618.

(21) Umehara, T.; Nakamura, Y.; Wakamori, M.; Ozato, K.; Yokoyama, S.; Padmanabhan, B. Structural implications for K5/K12-di-acetylated histone H4 recognition by the second bromodomain of BRD2. *FEBS Lett.* **2010**, *584*, 3901–3908.

(22) Vollmuth, F.; Blankenfeldt, W.; Geyer, M. Structures of the dual bromodomains of the P-TEFb-activating protein Brd4 at atomic resolution. *J. Biol. Chem.* **2009**, *284*, 36547–36556.

(23) Moriniere, J.; Rousseaux, S.; Steuerwald, U.; Soler-Lopez, M.; Curtet, S.; Vitte, A. L.; Govin, J.; Gaucher, J.; Sadoul, K.; Hart, D. J.

Krijgsveld, J.; Khochbin, S.; Muller, C. W.; Petosa, C. Cooperative binding of two acetylation marks on a histone tail by a single bromodomain. *Nature* **2009**, *461*, 664–668.

(24) The Structural Genomics Consortium. <http://www.thesgc.org>, 2011.

(25) Mujtaba, S.; Zeng, L.; Zhou, M. M. Structure and acetyl-lysine recognition of the bromodomain. *Oncogene* **2007**, *26*, 5521–5527.

(26) Bamborough, P.; Diallo, H.; Goodacre, J.; Gordon, L.; Lewis, T.; Seal, J. T.; Wilson, D. M.; Woodrow, M. D.; Chung, C. Fragment-Based Discovery of Bromodomain Inhibitors Part 2: Optimization of Phenylisoxazole Sulfonamides. *J. Med. Chem.* **2010**, *53*, 1021–1028.

(27) Hewings, D. S.; Wang, M.; Philpott, M.; Fedorov, O.; Uttarkar, S.; Filipakopoulos, P.; Picaud, S.; Vuppasetty, C.; Marsden, B.; Knapp, S.; Conway, S.; Heightman, T. D. 3,5-Dimethylisoxazoles act as acetyl-lysine-mimetic bromodomain ligands. *J. Med. Chem.* **2011**, *54*, 6761–6770.

(28) Congreve, M.; Chessari, G.; Tisi, D.; Woodhead, A. J. Recent developments in fragment-based drug discovery. *J. Med. Chem.* **2008**, *51*, 3661–3680.

(29) Schulz, M. N.; Hubbard, R. E. Recent progress in fragment-based lead discovery. *Curr. Opin. Pharmacol.* **2009**, *9*, 615–621.

(30) Hajduk, P. J.; Greer, J. A decade of fragment-based drug design: strategic advances and lessons learned. *Nature Rev. Drug Discovery* **2007**, *6*, 211–219.

(31) Hann, M. M.; Leach, A. R.; Harper, G. Molecular complexity and its impact on the probability of finding leads for drug discovery. *J. Chem. Inf. Comput. Sci.* **2001**, *41*, 856–864.

(32) Pan, C.; Mezei, M.; Mujtaba, S.; Muller, M.; Zeng, L.; Li, J.; Wang, Z.; Zhou, M. M. Structure-guided optimization of small molecules inhibiting human immunodeficiency virus 1 Tat association with the human coactivator p300/CREB binding protein-associated factor. *J. Med. Chem.* **2007**, *50*, 2285–2288.

(33) Swinney, D. C.; Anthony, J. How were new medicines discovered? *Nature Rev. Drug Discovery* **2011**, *10*, 507–519.

(34) Richon, V. M.; Emiliani, S.; Verdin, E.; Webb, Y.; Breslow, R.; Rifkind, R. A.; Marks, P. A. A class of hybrid polar inducers of transformed cell differentiation inhibits histone deacetylases. *Proc. Natl. Acad. Sci. U.S.A.* **1998**, *95*, 3003–3007.

(35) Dawson, M. A.; Prinjha, R. K.; Dittmann, A.; Giotopoulos, G.; Bantscheff, M.; Chan, W. I.; Robson, S. C.; Chung, C. W.; Hopf, C.; Savitski, M. M.; Huthmacher, C.; Gudgin, E.; Lugo, D.; Beinke, S.; Chapman, T. D.; Roberts, E. J.; Soden, P. E.; Auger, K. R.; Mirguet, O.; Doehner, K.; Delwel, R.; Burnett, A. K.; Jeffrey, P.; Drewes, G.; Lee, K.; Huntly, B. J.; Kouzarides, T. Inhibition of BET recruitment to chromatin as an effective treatment for MLL-fusion leukaemia. *Nature* **2011**, *478*, 529–533.

(36) Zuber, J.; Shi, J.; Wang, E.; Rappaport, A. R.; Herrmann, H.; Sison, E. A.; Magoon, D.; Qi, J.; Blatt, K.; Wunderlich, M.; Taylor, M. J.; Johns, C.; Chicas, A.; Mulloy, J. C.; Kogan, S. C.; Brown, P.; Valent, P.; Bradner, J. E.; Lowe, S. W.; Vakoc, C. R. RNAi screen identifies Brd4 as a therapeutic target in acute myeloid leukaemia. *Nature* **2011**, *478*, 524–528.

(37) Hinz, B.; Cheremina, O.; Brune, K. Acetaminophen (paracetamol) is a selective cyclooxygenase-2 inhibitor in man. *FASEB J.* **2008**, *22*, 383–390.

(38) Toussaint, K.; Yang, X. C.; Zielinski, M. A.; Reigle, K. L.; Sacavage, S. D.; Nagar, S.; Raffa, R. B. What do we (not) know about how paracetamol (acetaminophen) works? *J. Clin. Pharm. Ther.* **2010**, *35*, 617–638.

(39) Takehara, M.; Hoshino, T.; Namba, T.; Yamakawa, N.; Mizushima, T. Acetaminophen-induced differentiation of human breast cancer stem cells and inhibition of tumor xenograft growth in mice. *Biochem. Pharmacol.* **2011**, *81*, 1124–1135.

(40) Demont, E. H.; Garton, N. S.; Gosmini, R. L.; Hayhow, T. G.; Seal, J.; Wilson, D. M.; Woodrow, M. D. Tetrahydroquinoline derivatives and their pharmaceutical use. WO2011054841, 2011.

(41) Demont, E. H.; Gosmini, R. L. Tetrahydroquinoline derivatives as bromodomain inhibitors. WO2011054848, 2011.

(42) Bunnage, M. Chemical Probes for Epigenetics. Presented at the 4th International Symposium on Advances in Synthetic and Medicinal Chemistry, St. Petersburg, Russia, Aug 21–25, 2011.

(43) Nadin, A.; Hattotuagama, C.; Churcher, I. Lead-oriented synthesis: a new opportunity for synthetic chemistry. *Angew. Chem.* **2011**.

(44) Congreve, M.; Carr, R.; Murray, C.; Jhoti, H. A “Rule of three” for fragment-based lead discovery? *Drug Discovery Today* **2003**, *8*, 876–877.